JOURNAL OF MATERIALS SCIENCE 14 (1979) 1238–1244

# The metastable crystallization phases in the amorphous alloy METGLAS® 2826A

M. VON HEIMENDAHL, G. MAUSSNER
*Institut für Werkstoffwissenschaften I, Universität Erlangen-Nürnberg, Martensstr. 5, D-8520 Erlangen, Germany*

It is proved experimentally by transmission electron microscopy that the first crystallization of METGLAS® 2826A is a two-stage process, called MSI and MSII, rather than one-stage as described by Chang and Sastri. The details of MSI and MSII were investigated (structure, composition, morphology, activation energies) and discussed in terms of kinetics. MSI is controlled by small-scale diffusion involving metalloid depletion and, therefore, decelerated ($\sqrt{t}$-type) reaction kinetics; MSII grows linearly with $t$ because it is entirely interface-controlled. Certain differences in the results in comparison with Chang and Sastri's have been explained.

## 1. Introduction

Recently, Chang and Sastri [1] reported on the crystallization of the amorphous commerical alloy METGLAS® 2826A, $Fe_{32}Ni_{36}Cr_{14}P_{12}B_6$, produced by Allied Chemical Corp, Morristown N.J., USA. At the same time, in our laboratory, a detailed transmission electron microscopic (TEM) study was carried out on the same material which led only partially to similar results, but in some parts distinctly differed from Chang and Sastri's results. The latter is true especially with regard to the temperature range between 350 and 400° C during isothermal annealing, and up to 450° C during dynamic annealing. Here we found two different metastable crystallization stages (called MSI and MSII) in the TEM microstructure and correspondingly two separated peaks in the DTA, whereas in [1] only one peak and one crystallization stage is reported in this temperature range. Some other minor differences were found here and possible explanations for these are discussed in this paper. (For supplementary details, our Brighton conference paper [2] should be consulted.)

## 2. Experimental details

Specimen annealing was performed in evacuated quartz tubes only at temperatures higher than 500° C. For the lower temperatures, important in crystallization experiments, we used a commercial salt bath (as common in steel technology) because of the much better heat transfer and temperature control. No chemical attack was recognizable on the ribbon after the salt bath annealings. An interaction of the cations of the salt bath ($KNO_3$ + $NaNO_3$) at 350 to 400° C with the cations of the METGLAS appears to be unlikely. Two reasons account for this: an ion exchange between the monovalent cations $K^+$ and $Na^+$ and the polyvalent cations of the METGLAS is impeded for steric reasons, and moreover the mobility of polyvalent cations is too small to cause significant chemical changes of the ribbon surface.

For TEM, pieces of about 2 to 3 mm long were broken from the METGLAS ribbon, carefully ground with fine emery paper (grade 600) and jet-polished in a Tenupol apparatus. Whereas Chang and Sastri used 63.5 g $CrO_3$, 333 ml acetic acid, 10 ml $H_2O$ and 3 ml $HClO_3$ as electrolyte, we used concentrated acetic acid plus perchloric acid (grade 63%) in the volume ratio 10:1, employing 40 V at 7 to 8° C. Freshly mixed electrolyte should be kept 2 to 3 days before use, but should not be older than two weeks. Thinning took about 1 min from the ribbon which was initially 70 $\mu$m thick. Statistically, only one specimen out of four was useful in terms of transparency for 100 kV electrons. If the discs were too small to block the

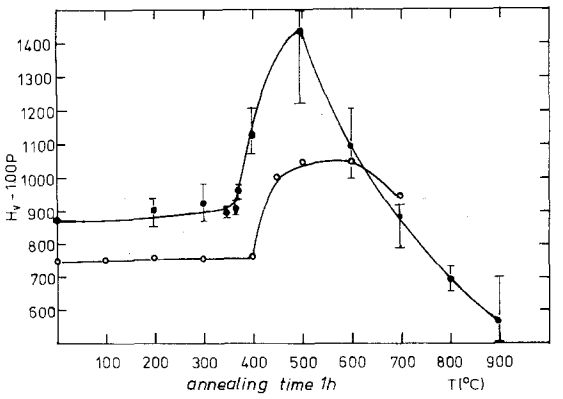


*Figure 1* Microhardness versus temperature (isochronic annealing for 1 h). Black symbols, own measurements; circles, [1].

light beam used for automatic voltage shut-off, an additional small Pt foil disc having a concentric 1 mm hole was mounted in the sample holder. A Philips EM 300 electron microscope, equipped with tilt-rotation specimen stage, was used for the TEM.

## 3. Results

Thermal differential analysis [1, 2] and microhardness measurements revealed the crystallization process to start at $\approx 350°$ C with isothermal annealing and at $\approx 420°$ C with dynamic annealing. In Fig. 1 microhardness versus time is shown in our isochronal annealing (1 h) in comparison with the continuous heating curve due to Chang and

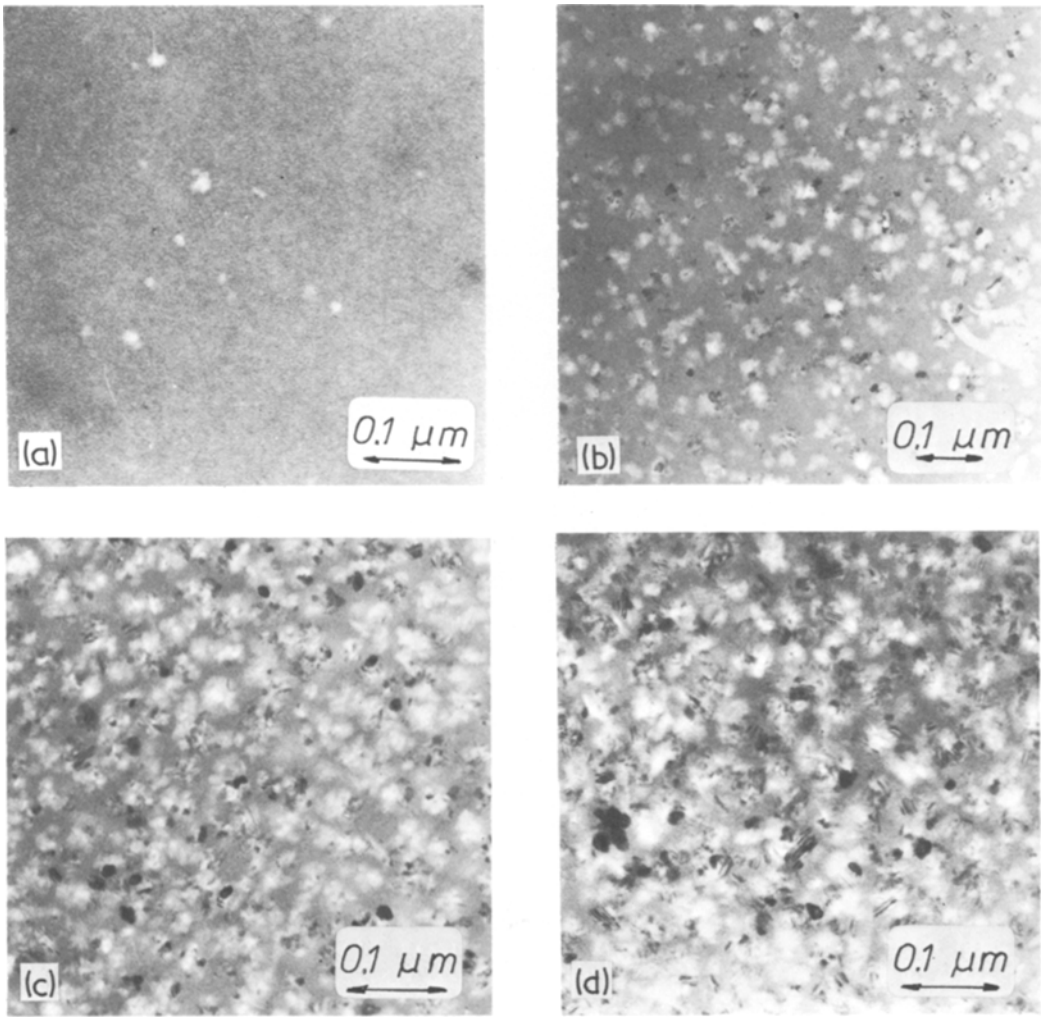


*Figure 2* Isothermal MSI crystallization at 375° C, TEM microstructure (bright-field). (a) 10 min, (b) 30 min, (c) 1 h 34 min, (d) 8 h.

TABLE I Crystallization phases in METGLAS® 2826A

| Phase | Structure | Composition | Size and temperature range (isothermal annealing) | Apparent activation energies ($kJ\ mol^{-1}$) |
|---|---|---|---|---|
| MSI | f c c<br>0.359 nm<br>± 0.002 | Ni/Fe solid solution [5] about 53:47 | ⩽ 30 nm<br>350–375° C | 270 (nucleation and growth by TEM from volume fraction [2])<br>360 for growth alone (from size of crystals at 3 temps.)<br>250–270 from DTA peak shift [2]<br>320 according to Drijver [4] (isothermal DTA) |
| MSII | b c t ($\epsilon_1$)<br>$a = 0.895$ nm<br>$c = 0.438$ nm<br>± 0.003 | $Ni_3P$-type resp. $(Ni, Fe, Cr)_3$ (P, B) | ⩽ 500 nm<br>390–420° C (and above) | 450 from growth versus time (TEM Fig. 4)<br>450 from line intersection technique [2] |
| SIII | 1. f c c<br>0.357 nm<br>2. b c t ($\epsilon_1$)<br>$a = 0.900$ nm<br>$c = 0.444$ nm<br>3. probably $\beta$ [1], but ordered [10] | similar above MSI<br>Ni-, Fe-rich, Cr-reduced $(Ni, Fe, Cr)_3$ (P, B)<br>Cr- and P-rich (the lengthy inclusions from Fig. 4 in [2] | 1–3 $\mu$m<br>⩾ 600° C | 180 from DTA peak shift [2, 10] |

Sastri [1]. That the hardness increase starts earlier and increases more in our measurements is probably due to the fact that we annealed up to 415° C directly in a salt bath and only from 500° C in evacuated quartz tubes. So a direct and immediate heat transfer was guaranteed for the lower temperatures which plays a role in the short annealing times. In [1] the continuous heating was done in the pure argon atmosphere of the DSC cell. In any case, the curves indicate the crystallization to start at the temperature quoted above.

To prove the two-stage initial metastable crystallization as seen from the double peak in the DTA (Fig. 1 in [2]), specimens annealed isothermally at 375 and 396° C were studied by TEM. After 10 min at 375° C, only very few crystals had grown in the glassy matrix (Fig. 2a). After 30 min, considerably more crystals, only slightly increased in size, appeared (Fig. 2b). In these bright-field images the crystals appear brighter than the amorphous matrix (explicable in terms of general scattering theory, e.g. [3]) and diffuse at their edges. However, crystal contours are absolutely sharp if they are accidentally Bragg-oriented and, therefore, appear dark in bright-field. With increasing time (Fig. 2c and d) the number of crystals increases but their size increases only very little. Thus, the reaction seems to be predominantly nucleation-controlled and growth is very limited. Electron diffraction and X-ray microanalysis in combination with STEM [5] of these MSI crystals revealed their structure and composition to be as shown in Table I.

The second crystallization stage, MSII, is illustrated in the isothermal annealing sequence at 396° C reproduced in Fig. 3, and is clearly distinguished from MSI. Closer examination reveals that the very small, dendritic MSI crystals which have been nucleated first are not dissolved, but remain and become enclosed by the much bigger MSII (cf. Fig. 3 in [2]). Again, in bright-field those crystals which happen to be Bragg-oriented appear black with sharp contours. Their size was measured in relation to time and is given in Fig. 4 for two temperatures. The values refer to the mean value of the largest crystals taken from several TEM photographs. In contrast to MSI, growth occurs linearly until the whole original glass volume is transformed into the crystalline state as is the case in Fig. 3 of [2].

At much higher temperatures, starting at about 600° C, a total recrystallization of the whole structure proceeds, leading to the final (equilibrium) stable stage, called SIII. It is scarcely of technical importance and is described in [2]. Also the kinetics and activation energies of MSI and MSII gained from quantitative TEM metallography are included there.

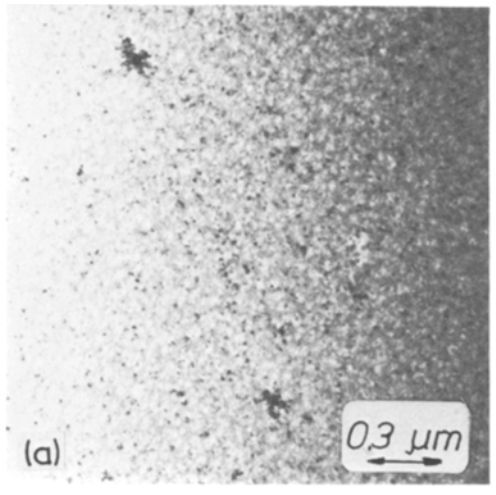


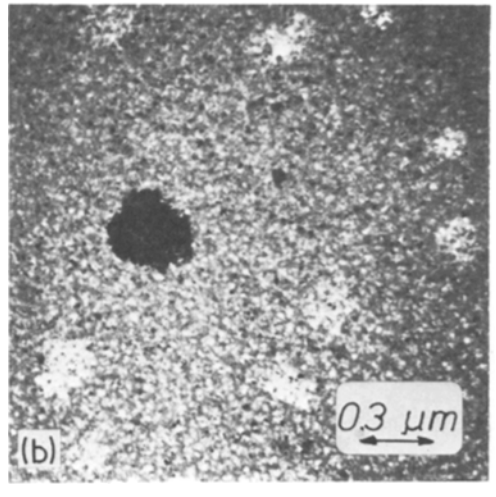


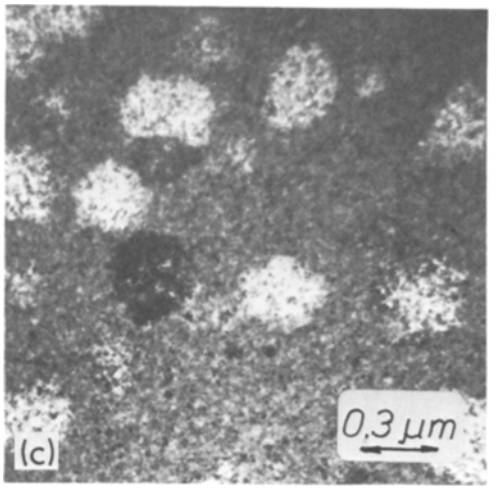


*Figure 3* Isothermal growth of MSII crystals at 396° C, TEM microstructure (bright-field). (a) 20 min, (b) 64 min, (c) 93 min.

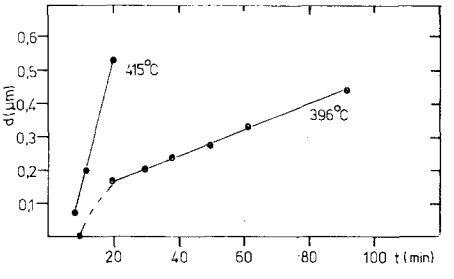


*Figure 4* Growth of MSII crystals (maximum diameters) versus time in isothermal annealing.

## 4. Discussion

### 4.1. General

The elemental analysis of the tiny, first formed MSI crystals was possible by means of X-ray microanalysis in STEM and is described in detail elsewhere [5]. The result was that during the MSI crystallization, the metalloid P (and probably also B) and also a considerable fraction of Cr is removed; thus the MSI crystals consist of Ni and Fe solid solution (Ni-rich). This is in accordance with the fcc lattice constant determination of 0.359 nm obtained independently by electron diffraction [2]. Drijver *et al.* [4] found nearly the same value, 0.358 nm, and noticed that this value agreed with the Ni/Fe solid solution lattice constant for an Ni/Fe relation of 53:47 which is the same as in the original METGLAS material, namely 36:32.

Since P and Cr are not involved in the MSI crystallization*, this fact explains two of the main experimental observations described above:

(i) The slow growth of MSI. The small-scale diffusion necessary for P, Cr (and probably also B) determines the reaction, leading to a $\sqrt{t}$ growth law for the individual crystal diameters. The copious nucleation, as seen in Fig. 2, mainly determines the transformed volume fractions (Fig. 7 in [2]).

(ii) The necessity of the distinct, subsequent MSII stage. Owing to the P-, Cr- and probably B-depletion of the MSI crystals, the glassy residual matrix is more and more enriched in these components and must later crystallize into another

*These elemental changes on crystallization mean it is "primary" in the terminology of Köster [6], whereas in a "polymorphous" crystallization, the elemental composition stays the same. This depends on the specific free enthalpy versus concentration diagram of the alloy (cf. Fig. 9 in [7]).

phase, rich in these elements. The observed $\epsilon_1$-type structure of MSII, having a metalloid/metal ratio of 1:3, satisfies this requirement. The MSII crystals grow proportionally to $t$ (Fig. 4), this reaction then being entirely interface-controlled (no further diffusion necessary). (Nucleation of MSII is probably very easy at the phase boundaries between already existing MSI crystals and the glass matrix.)

## 4.2. Activation energies

A critical assessment of the analysis from Fig. 4 to yield the growth activation energy of 450 kJ mol$^{-1}$ for MSII was performed as follows. The usual Arrhenius law for thermally activated processes was applied, growth velocity, $v$, being proportional to $\exp(-Q/RT)$. A small inaccuracy of ±5% in the slope of the straight lines in Fig. 4 gives an error of only 10 kJ mol$^{-1}$. However, an error of just ±1° C in the temperature measurement or control of the furnace yields a 25 kJ mol$^{-1}$ change in the activation energy, $Q$ (both referred to the 450 kJ mol$^{-1}$ value from this case). Therefore, careful furnace control and temperature homogeneity within the salt bath is very important for these experiments. $Q$ for MSII growth was obtained here from only two temperatures. For a better determination of $Q$ and confirmation that an Arrhenius law is obeyed, more temperatures need to be empolyed. This will be undertaken in future.

In the present case of MSII, an independent determination of the activation energy was achieved by the line intersection technique of quantitative metallography. The volume fraction of MSII crystals was determined versus time at constant temperatures by measuring the relative area of MSII in the TEM photographs, assuming these crystals are considerably larger than the foil thickness, which was the case. The result was again 450 kJ mol$^{-1}$ (cf. Table I.)

The first value for the activation energy of 270 kJ mol$^{-1}$ for MSI, as given in Table I was reported earlier [2]. It referred to the sum of nucleation and growth, since it was obtained from TEM volume fractions of the total phase amount at each time and temperature. Basically, those techniques are inferior which use properties (such as DTA, length changes, metallographic volume fractions, etc.) giving the combined effect of several contributions, such as nucleation and growth. Meanwhile, a separated estimation of the activation energy of growth exclusively could be achieved as follows. The size of the largest MSI crystals were 25 nm after 6 h at 350° C (Fig. 1 in [5]), 20 nm after 1 h at 358° C and 15 nm after 10 min at 375° C (Fig. 2a). (The smaller crystals were probably the result of a later nucleation.) We assume diffusion control of the process. Although it is not certain whether we have an exact $\sqrt{t}$ proportional growth, for a first, rough guess we may calculate the effective diffusion coefficients, $D$, from the sizes $s$, after the times, $t$, as $s^2 = 2Dt$. Using the values at the three temperatures given above, an Arrhenius plot of $\ln D$ versus $1/T$ may be drawn. The result for the activation energy from the slope is ≈360 kJ mol$^{-1}$*). This is higher than the 270 kJ mol$^{-1}$ for nucleation and growth together. This is reasonable insofar as it was observed (see above) that MSI nucleation is copious, growth however being restricted; i.e. it is to be expected that the value for growth is higher than that for nucleation alone or for the sum of both effects. The values determined earlier from DTA [2, 4] refer obviously to the sum of nucleation and growth and differ by ±10% taking 290 kJ mol$^{-1}$ as a mean value from [2] and [4]. Generally, the values reported may be taken only as preliminary with restricted accuracy; in addition, the complication of certain differences from batch to batch may play a role. More work needs to be done.

The slope of the Johnson–Mehl–Avrami plot, Fig. 8 in [2], was $n = 1.7$. This time exponent is in accordance with growth of approximately spherical particles for MSI. The TEM pictures in Fig. 2 show them as being roughly sphere-like, and partly dendritic.

## 4.3. Relation to the work of Chang and Sastri [1] and others

The fact that Chang and Sastri did not observe the two-stage metastable behaviour by TEM and only one DTA peak around 450° C is probably due to two circumstances: (i) the higher heating rates used in their dynamic DTA run, and (ii) the fact that in the isothermal annealing used for their

*This method is similar to the so-called "method of standard results" [8] using different times to reach the same particle structure at different temperatures. It is preferable in comparison to isothermal measurements of particle diameters versus time, which is inaccurate and difficult if particles are very small and slowly growing as in the case of MSI.

TEM sequence at 400° C they sealed the samples in evacuated quartz capsules, whereas we used a salt bath. Especially during the short anneals of a few minutes, their samples probably did not attain the full time–temperature (rectangular) profile. Therefore, the isothermal 400° C series in the TEM of Chang and Sastri look like ours at lower temperatures about 20 to 30° C, i.e. essentially still being MSI.

In our investigation, all the structural data from Table I were gained from selected-area diffraction and related dark-field electron microscopy technique [9] of the relevant phases [10] or by STEM with EDS [5]. On the other hand, in the case of electron diffraction the lattice parameter resolution is poorer than in the X-ray case, of course. Thus, we have been unable to differentiate between the $\gamma$ and $\eta$-phases of Chang and Sastri, which differ in parameter by only 0.002 nm. Also $\alpha$ and $\theta$ were not found in our investigation.

Little information is available so far about 2826A. Drijver *et al.* [4] report on the stability and mechanical properties of METGLAS 2826A, essentially dealing with creep and fatigue tests below the crystallization temperature. They did not include TEM investigations, but report on activation energy measurement by isothermal DTA for the first crystallization stage to be 320 kJ $mol^{-1}$. This value is in reasonable agreement with ours (cf. Section 4.2 and Table I).

It is interesting to compare the results of this work with that of Walter and Bartram [12] on the iron-based amorphous alloys $Fe_{84}B_{16}$ and $Fe_{73}Co_{10}B_{17}$. These alloys also exhibit a two-stage crystallization similar to MSI and MSII. But the first stage in [12] are small b c c ($\alpha$)-iron crystals, of course, (and not f c c as in our case of Ni-base alloy), later surrounded (occluded) by $Fe_3B$ crystals having a similar crystal structure as the b c t $Fe_3P$. However, if the metalloid content is increased by only a few per cent, reaching 20% as in $Fe_{80}B_{20}$ or $Fe_{50}Ni_{30}B_{20}$, the crystallization behaviour is changed drastically: only b c t $Fe_3B$ nucleates and grows in one stage, having a characteristic eutectic, cellular microstructure [12]. The latter was also investigated and described in detail by Herold and Köster [14] for $Fe_{80}B_{20}$. The same behaviour, differing basically from 2826A, is shown in the METGLAS 2826 = $Fe_{40}Ni_{40}P_{14}B_6$ [12, 13], which also contains 20% metalloid and no Cr in contrast to 2826A. Walter and Bartram therefore conclude that it is "the metalloid which determines the type, shape and structure of crystals formed by crystallization of amorphous alloys containing various amounts of B and P" [12]. This idea is in agreement with the results of Köster and Herold [15], investigating the influence of metal or metalloid variations on crystallization of amorphous Fe–B alloys in terms of free energy versus concentration diagrams.

Concerning the two-stage metastable crystallization, similar behaviour was reported by Boswell [16] with regard to $(Ni, Pd)_{82}P_{18}$. This alloy also showed first a volume–diffusion-controlled MSI stage, followed by an interface-controlled MSII reaction with a larger activation energy than MSI. Again, it is noteworthy that in this case [16] the alloy contained only 18% metalloid and not 20%.

Further work in our laboratory will include the dependence of the results on the local position within the ribbon (e.g. [11]), the influence of superimposed mechanical stresses and of alloy variations (in relation to the Cr-free METGLAS® 2826 [12]).

## Acknowledgements

We appreciate fruitful relevant discussions with Dr H. A. Davies, England, Dr A. L. Mulder, Holland, Dr H. Schaeffer and Dr U. Köster, Germany and Dr P. H. Shingu, Japan. A critical reading of the manuscript by Professor Dr B. Ilschner is gratefully acknowledged. The authors are also grateful to Miss G. Gunesakera for critical reading and correcting the English version of the manuscript.

## References

1. H. CHANG and S. SASTRI, *Met. Trans.* 8A (1977) 1063.
2. M. VON HEIMENDAHL and G. MAUSSNER, Proceedings of the International Conference on Rapidly Quenched Metals, University of Sussex, Brighton, England, 3–7 July 1978, Vol. 1 (Metals Soc., London, 1978) p. 424.
3. L. REIMER, "Elektronenmikroskopische Untersuchungs- und Präparationsverfahren" (Springer-Verlag, Berlin, Heidelberg, New York, 1967) Ch. 6.6.
4. J. W. DRIJVER, A. L. MULDER, W. C. EMMENS and S. RADELAAR, in [2].
5. M. VON MEIMENDAHL and H. OPPOLZER, *Scripta Met.* **12** (1978) 1087.
6. U. KÖSTER, *Acta Met.* **20** (1972) 1361.
7. H. WARLIMONT, *Z. Metallkd.* **69** (1978) 212.

8. T. EVANS and E. WILLIAMS, *Phil. Mag.* **20** (1969) 181.
9. M. VON HEIMENDAHL, "Einführung in die Elektronenmikroskopie" (Vieweg-Verlag, Braunschweig, 1970).
10. G. MAUSSNER, Diploma Thesis, Universität Erlangen-Nürnberg, 1978.
11. A. S. SCHAAFSMA, H. SNIJDERS and F. VAN DER WOUDE in [2].
12. J. L. WALTER and S. F. BARTRAM, *ibid.*
13. J. L. WALTER, P. RAO, E. F. KOCH and S. F. BARTRAM, *Met. Trans.* **8A** (1977) 1141.
14. U. HEROLD and U. KÖSTER, *Z. Metallkd.* **69** (1978) 326.
15. U. KÖSTER and U. HEROLD, in [2].
16. P. G. BOSWELL, *Scripta Met.* **11** (1977) 701.

Received 29 August and accepted 6 October 1978.